

energy level gap in the absorber and resonant absorption will be at a maximum. For a source and absorber which are chemically identical this relative velocity will be zero. Application of an additional velocity increment will lower the resonant overlap and decrease the absorption. Application of a sufficiently large relative velocity will destroy the resonance completely.

A Mössbauer spectrum comprises a series of measurements at different velocities (that is energies) across the resonant region. The convention universally adopted is that a closing velocity between source and absorber (i.e. a higher energy) is defined as positive.

It has already been shown in Chapter 1 that the resonant absorption curve for an ideally thin source and absorber has a width at half-height Γ_r , which is twice the Heisenberg width of the emitted γ -photon. The Doppler velocity v corresponding to this energy Γ_r is given by

$$\frac{v}{c} = \frac{\Gamma_r}{E_\gamma}$$

where c is the velocity of light. Typical numerical values for commonly used Mössbauer isotopes are

^{57}Fe (14 keV)	0.192 mm s^{-1}	^{119}Sn (24 keV)	0.626 mm s^{-1}
^{127}I (58 keV)	2.54 mm s^{-1}	^{125}Te (35 keV)	5.02 mm s^{-1}
^{195}Pt (99 keV)	16 mm s^{-1}		

A full list of such values in Appendix I shows that the velocities range from 3.1×10^{-4} for ^{67}Zn up to 202 mm s^{-1} for ^{187}Re . They are all very small when compared with the tremendous velocities ($\sim 7 \times 10^5 \text{ mm s}^{-1}$) used by Moon in 1950 to detect nuclear resonance fluorescence without recoilless emission, and show dramatically that the Mössbauer technique eliminates both recoil and thermal broadening. The Heisenberg relation means that an excited state with a shorter half-life has a greater uncertainty in the γ -transition energy and hence a broader resonance line.

Since the Doppler energy shift is relative to the source and absorber only, it is independent of the frame of reference. In practice one resonant matrix is maintained at rest. For transmission experiments it is usually more satisfactory mechanically to move the source. It is then much easier to change absorbers and to vary their temperature. The only major problem is that the source of the γ -rays and the detector are then not at rest relative to each other, and the solid angle subtended by the source varies during the motion. If the amplitude of the source motion is large, a correction term should be applied. There is also a limitation on the counting geometry since the Doppler shift $E_\gamma v/c$ is only accurate along the axis of source motion. A γ -photon travelling to the detector at an angle θ to this axis will have an effective Doppler shift of $E_\gamma v \cos \theta/c$. A large solid angle in the counting geometry will thus cause a distortion in the shape of the Mössbauer absorption line.

[Refs. on p. 43]

The difficulty can be overcome by maintaining an adequate separation between source and detector or by collimation of the γ -ray beams.

There are two general approaches to the measurement of γ -ray transmission at different Doppler velocities:

- (a) measurement of the total number of transmitted γ -photons in a fixed time at a constant velocity, followed by subsequent counts at other velocities; in this way the spectrum is scanned stepwise one velocity at a time;
- (b) rapid scanning through the whole velocity range and subsequent numerous repetitions of this scan, thereby accumulating all the data for the individual velocities essentially simultaneously.

The relatively low photon flux-density necessitates much longer counting times to achieve significant counting statistics than, for example, in optical spectroscopy. The statistical behaviour of the γ -emission results in a standard deviation of \sqrt{N} for a total number N of registered γ -counts. Hence the standard deviation in 10,000 counts is 100 (1%); in 1,000,000 counts is 1000 (0.1%). The longer the counting time, the better the definition of the resonance line, but the improvement to be gained must be balanced against the experimental time required and the long-term stability or reproducibility of the apparatus.

2.2 Constant-velocity Drives

To move an object at a constant velocity with high reproducibility and stability, when it is restricted by both a relatively small amplitude of movement and the necessity for repetitive motion, is a difficult problem in applied mechanics. Several constant-velocity spectrometers have been described, and these can be briefly classified under eight different headings. A simple diagram of each type is shown in Fig. 2.1 and references to more detailed descriptions are given where available.

- (i) lathe and gears: a lead screw parallel to the γ -ray axis is used to drive the source, the velocity being varied by use of gears or a variable-speed motor [3, 4].
- (ii) lathe and inclined plane: the lead screw is perpendicular to the γ -ray axis and is driven by a constant-speed motor. The source is moved by a slide-plate on an inclined plane mounted on the lead screw carriage and the velocity is varied by altering the angle of inclination of this plane [5].
- (iii) hydraulic devices: the driving force is provided by hydraulic pressure. A typical system embodies a double-action cylinder to enable continuous repetitive movement [6].
- (iv) cam and gears: a wide variety of rotating cam drives has been used. The exact shape of the eccentric determines the motion of the follower [7]. One of the more recent instruments uses a 70-kg rotating disc mounted with its axis vertical [8]. It features a helicoidal surface on the outer circumference

[Refs. on p. 43]

transmitting a linear velocity to a piston aligned vertically and gliding on the surface.

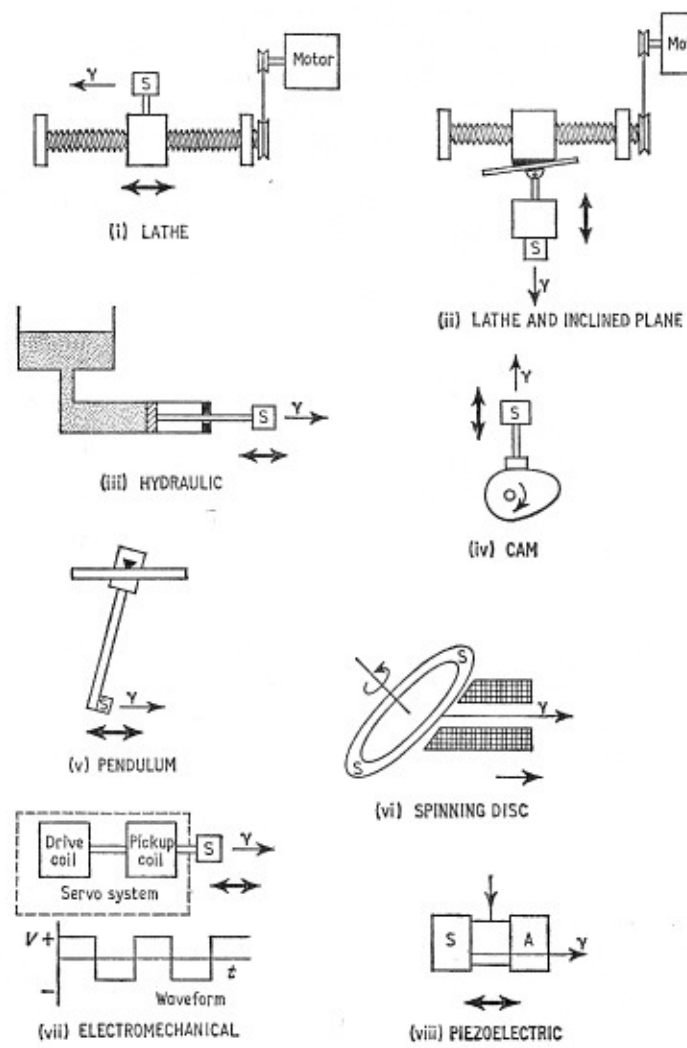


Fig. 2.1 Eight drive systems for producing constant velocities. The direction of motion is indicated by the heavy arrow. The source is labelled S.

(v) pendulum: a long pendulum device gives a good approximation to constant velocity at the bottom of its swing and can be activated by an electromagnetic drive coil [9, 10].

(vi) spinning disc: an accurately driven rotating disc can be used, the Doppler velocity along the γ -ray axis being varied by altering the speed of rotation, the diameter of the disc or its inclination.

[*Refs. on p. 43*]

(vii) electromechanical drive: an electromechanical servo-drive can be driven with a square wave to give a constant velocity [11, 12].

(viii) piezoelectric drive: a triangular voltage waveform applied to a piezoelectric crystal which is glued in between source and absorber produces alternate forward and backward constant velocity [13].

The only other essential equipment in these constant-velocity spectrometers comprises a γ -ray detection system, a timer, and a scalar for registering the accumulated count at each successive velocity.

The advantages offered by a constant-velocity spectrometer include the ability to examine a small velocity range not centred on zero velocity, and to calibrate the instrument directly in terms of absolute velocity. It is also often considered to be less expensive than the alternative velocity-sweep techniques considered in Section 2.3, but this probably applies only to simple demonstration equipment. A constant-velocity instrument of any precision must involve considerable expense in machine-shop and development time.

There are many disadvantages. Such an instrument is extremely tedious to operate unless it has been fully automated (with considerable increase in expense). It is difficult to machine cams and lead screws to the precision required to give an accurately linear drive. Mechanical wear and vibrations are inevitably a problem. The velocities attainable are limited to the range $0.1\text{--}10 \text{ mm s}^{-1}$. Cam and lead screw drives require a complicated automatic reversing system with rejection of all counts received at the end of the travel when the velocity is changing. The solid angle and cosine effects have already been referred to though they can be minimised by moving the absorber rather than the source. Rotating discs make very inefficient use of the resonant matrix because this must be distributed over a large annulus rather than in a small area. Finally, if the source activity is short-lived compared with the experimental time-scale, the observed count rates over successive constant intervals of time must be corrected for the decreasing rate of γ -emission.

The cumulative result of these disadvantages has been to restrict the continued development of constant-velocity spectrometers. One of the few major developments of recent years has been the description of an instrument which takes readings at a number of velocities pre-programmed on a length of punched tape [14]. The great majority of investigations are now made using repetitive velocity-scan systems.

2.3 Repetitive Velocity-scan Systems

Mechanical drives can be very tedious to operate (unless they are very fully automated) because of frequently having to alter the velocity setting. The availability of small, transistorised, multichannel analysers embodying typically 400 or 512 individual scalars in a computer-type memory store prompted de Bennedetti to suggest their use for Mössbauer data acquisition

using repetitive scanning techniques. The Doppler motion is provided by an electromechanical drive system which is controlled by a servo-amplifier. The amplifier is fed with a reference voltage waveform which repeats itself exactly with a frequency of between about 5 and 40 Hz ($1 \text{ Hz} = 1 \text{ cycle s}^{-1}$). The actual drive or transducer embodies two coils, one of which produces a voltage proportional to the *actual* velocity of the shaft. The servo-amplifier compares this signal to the reference waveform and applies corrections to the drive coil to minimise any differences. In this way, the centre shaft which is usually rigidly connected to the Mössbauer source executes an accurate periodic motion. A considerable volume of literature is available on the design of suitable transducers [15–22]. Velocities of over 600 mm s^{-1} can be achieved, or as low at $10^{-2} \text{ mm s}^{-1}$ [23]. Even smaller velocities can be obtained by a piezoelectric crystal glued between source and absorber, and in one instance has been used at speeds of up to about 8 mm s^{-1} [24].

Several types of command waveform have found favour, and three of these

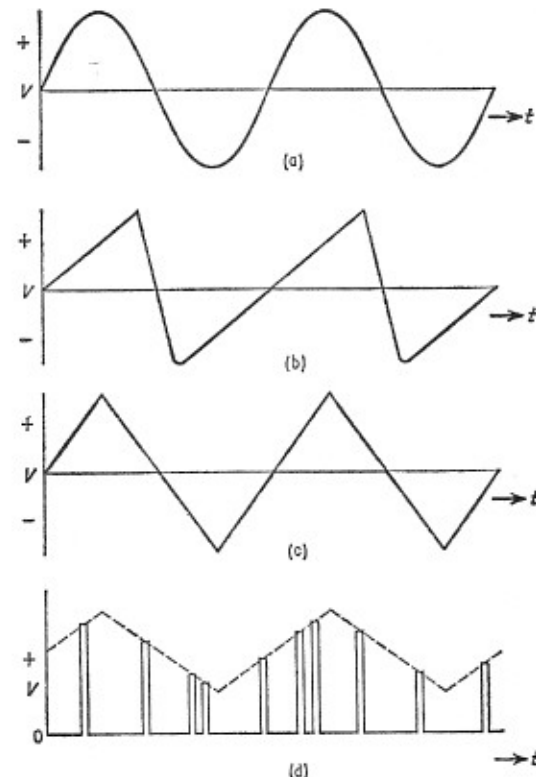


Fig. 2.2 (a), (b), and (c) show three of the most popular voltage waveforms for electromechanical drive systems. (d) illustrates how each detected γ -ray can be used to produce a pulse with amplitude characteristic of the instantaneous velocity.

[Refs. on p. 43]

are illustrated in Fig. 2.2. (Fig. 2.2d is discussed on pp. 23–24.) The sine wave (2.2a) is less demanding on the mechanical adjustment of the transducer, but since the velocity is directly proportional to the voltage it produces a markedly non-linear scale on the final spectrum. The asymmetric double ramp (2.2b) executes about 80% of the motion with a constant acceleration and therefore a linear velocity scale, but the high-frequency components cause some difficulties. The symmetrical double-ramp (2.2c) scans the spectrum alternately with constant acceleration in opposite directions, and in some equipment cuts by half the number of data units available and produces a double (mirror-image) spectrum; this can be folded to give an additional check on linearity.

Many spectrometers have been described, but most fall into one of three basic classes as follows:

(a) Pulse-height Analysis Mode

Many multichannel analysers have a facility known as pulse-height analysis, and a typical system employing an analyser in this mode is shown in Fig. 2.3. Several detailed descriptions are available [25–27].

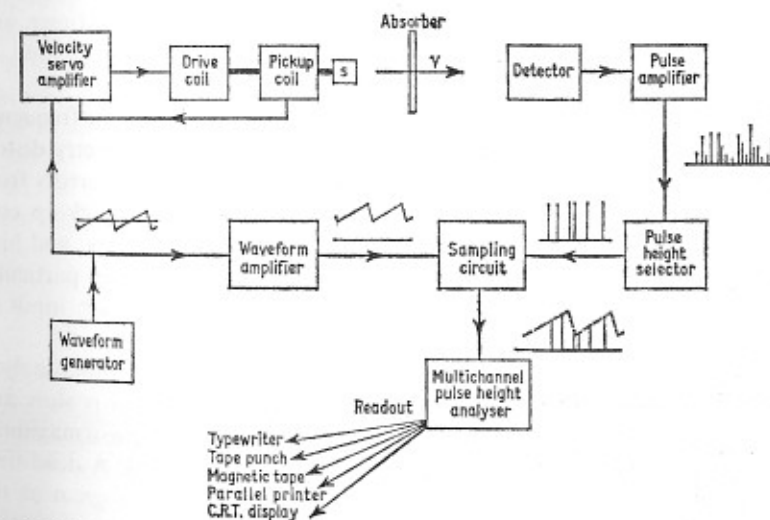


Fig. 2.3 Schematic arrangement for the pulse-height analysis spectrometer described in the text.

A reference waveform identical to that supplying the drive is given a d.c. shift such that it is always positive. When a γ -ray which has passed through the absorber is detected, the waveform is sampled so that a pulse is produced which has a voltage maximum characteristic of the instantaneous velocity of the source at the time of emission (see Fig. 2.2d). An analogue-to-digital

[Refs. on p. 43]

converter (A.D.C.) transforms this pulse into a train of pulses from a constant-frequency clock such that the number of pulses is proportional to the voltage. These pulses then sequentially step through the channel addresses of the analyser until the train is exhausted, at which point the number stored in the open channel is increased by one.

In this way each channel in the analyser will receive those γ counts which are registered in the narrow velocity range assigned to it, and in the cases of constant-acceleration waveforms such as 2.2b and 2.2c the channel number is directly proportional to the velocity. Many pulses are detected and stored during each cycle of the motion, and successive cycles over a long period of time allow the spectrum to build up as a whole. At velocities where resonance absorption occurs the accumulation rate will be slower. The analyser has a cathode-ray tube (C.R.T.) display in which a voltage proportional to the accumulated count of a channel is used as the vertical deflection, and a voltage proportional to the channel address number is used as the horizontal deflection. At the frequency of scan used in the experiments this gives a continuous visual display of all the channels. The spectrum can thus be inspected at any time during the course of a run. This is a significant advantage over constant-velocity instrumentation. No operator attention is required during the run which can, if desired, be terminated by automatic timer, and full digital readout is available to typewriter, paper tape, magnetic tape, or parallel-printer peripheral devices.

Other advantages are as follows: the use of a 40-Hz scanning frequency results in a very small amplitude of motion which reduces geometry distortions to negligible proportions for most nuclides and minimises errors from non-linearities in the voltage/velocity correspondence of the pick-up coil. Half-life corrections with short-lived sources are also unnecessary, and high velocities can be achieved at relatively small amplitudes. One particular system accumulates two spectra simultaneously using a common input to the analyser [28].

There are, however, two prime disadvantages of pulse-height analysis methods. The A.D.C. (analogue-to-digital-conversion) process is slow and each time a pulse is counted it imposes a variable 'dead time' up to a maximum of about 100 μs during which no other pulse can be accepted. A dead-time must therefore be fixed by the operator at a value at least as great as the maximum time for storage, otherwise one would register faster counting rates at the lower channel address numbers. The absolute counting rate of the analyser is thereby limited to 10^4 pulses per second for normal 1 μs pulses. The second difficulty concerns the relatively poor linearity and stability of an A.D.C. unit. A differential linearity of $\pm 1\%$ is normal and $\pm 0.2\%$ can be achieved with some difficulty. However, this means a potential variation of 1% of the baseline across the final spectrum on which may be superimposed a Mössbauer resonance of the same order of magnitude.

[Refs. on p. 43]

This presents a difficulty if the data are to be analysed by computer and it reduces the feasible accuracy of measurements.

Both these objections can be overcome by using a time-mode system and spectrometers based on this latter principle have now virtually replaced those operating in the pulse-height analysis mode.

(b) Time-mode (Multiscalar-mode) Spectrometers

The time-mode system dispenses entirely with the A.D.C. processing. The channel address is advanced sequentially under the control of a very accurate crystal oscillator with a dwell time in each channel of say 50 or 100 μs . While a channel is open it accepts all input pulses from the detection system. The only dead-time is that incurred during the channel advance, and this is only 5–10% of the total time. In this way count-rates approaching 10^6 s^{-1} can be achieved. The baseline constancy is directly dependent on the short-term (one period of the drive) stability of the crystal oscillator. Usually it is good enough not to present any problems, and the biggest potential non-linearity is from geometric effects when using high-velocity scans.

The servo-controlled transducer system is identical to that used in the pulse-height analysis mode, but it must be coupled to the channel advance frequency. Several variations have been proposed for this. Some workers have built their own waveform and channel advance circuitry. Others have taken an existing analogue voltage, proportional to the channel address, from an analyser using its own internal crystal oscillator, and have used this as the drive reference signal for a waveform of type shown in Fig. 2.2b. A schematic layout is given in Fig. 2.4. The 'staircase' nature of the signal is smoothed by the servo system to produce a constant acceleration over 80% of

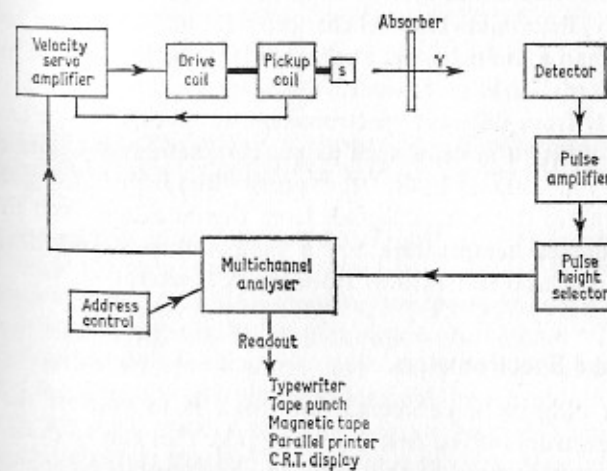


Fig. 2.4 Schematic arrangement for a time-mode spectrometer.

[Refs. on p. 43]

the scan. A third method has been to take a signal from an internal bi-stable of the analyser and produce a double ramp as in Fig. 2.2c. Several detailed descriptions of time-mode operation are available [12, 29–32].

A more recent innovation which is only completely satisfactory if the transducer unit is of high quality is to use forward-backward address scaling [33, 34]. While the source executes one period of a symmetrical double-ramp waveform as in Fig. 2.2c the channel addresses are stepped once in a forward and once in a backward direction. The result is a superposition of forward and backward scans and the accumulation of only one spectrum. This method would suffer if the return scan were not the mirror-image of the forward, but otherwise it has the advantages of allowing more efficient use of the channel storage and a reduction in geometry effects. An alternative approach [35] is to activate the analyser for $\frac{1}{2}$ or $\frac{1}{4}$ of the double-ramp cycle thereby doubling or quadrupling the effective resolution. The prime disadvantage of these modifications is a considerable increase in 'dead-time', necessitating longer counting times.

(c) On-line Computers

A recent development which should see more widespread application in the next decade is the use of small on-line computers. Typically these contain a memory of 4096 (4k) 12-bit words and a typical arrangement has already been described in some detail [36, 37]. The pick-up voltage which is a direct measure of velocity is digitised by an A.D.C. unit. Since this voltage varies slowly, a continuous and accurate value of the voltage can be stored by the computer. When the digital equivalent of the voltage changes by a pre-defined increment, the channel address for data storage is altered. This differs from the time-mode system where the input waveform (and not the actual velocity) determines channel changeover. Since a 4k-store computer is much larger than a multichannel analyser it is possible to utilise much more of the computer's facilities. Several Mössbauer spectra can be accumulated simultaneously from different spectrometers, or storage space can be used with entirely different systems such as gas-chromatography data collection, possibly on a time-sharing basis. Other possibilities include using the A.D.C. facility to monitor the voltage signals from thermocouples and to maintain a pre-programmed temperature via a temperature-control device which receives its command instructions from the computer.

2.4 Derivative Spectrometers

A somewhat different experimental approach is to convert the resonant absorption spectrum into its first derivative [38]. This can be done by a similar modulation procedure to that used in electron-spin resonance spectrometers. The major complication is that two modulating velocity terms are

required, a constant velocity v_0 and a high-frequency, low-amplitude, periodic velocity of sinusoidal type. The resultant velocity is then

$$v = v_0 + k \sin \omega t$$

The transmission $\tau(v)$ is now given by

$$\tau(v) = \tau(v_0 + k \sin \omega t)$$

which for appropriate values of the amplitude k and frequency ω approximates to

$$\tau(v_0, \omega) = k \frac{d\tau}{dv_0} \sin \omega t$$

Thus $\tau(v_0, \omega)$ is proportional to $d\tau/dv_0$, the derivative of the normal transmission curve. The amplitude of the secondary modulation must be much less than the width of the Mössbauer line so that $d\tau/dv_0$ is nearly constant over the amplitude.

Bressani, Brevetto, and Chiavassa have described an instrument using this feature [39]. The absorber is moved with a constant velocity v_0 and the source with varying velocity $k \sin \omega t$. The detected γ pulses are not distributed statistically but are periodically bunched by the extra modulation. A lock-in amplifier can be made to respond to the bunching frequency and with a suitably long integration time will produce a voltage proportional to $d\tau/dv_0$.

A resultant spectrum is shown in Fig. 2.5 where it is compared with the normal transmission spectrum. The method has the advantage of being more selective in the presence of strong background radiation since the latter will not have a time distribution containing the modulation frequency. However, strong sources are required to obtain the best results, and it is unlikely that the technique will ever replace the very popular velocity-scan systems.

2.5 Scattering Experiments

Although the most usual method of registering a Mössbauer spectrum is by a transmission experiment, it is also possible to observe the resonance by a scattering method [40–43]. γ -rays can be scattered by several mechanisms. The electrons in the atoms can scatter the incident γ -rays without change in the wavelength (Rayleigh scattering) or with an increase in the wavelength (Compton scattering). The corresponding processes in which the nucleus is the scattering agent are usually weak enough to be neglected. There are also the γ -rays produced by recoilless and non-recoilless nuclear resonance scattering. The Rayleigh and resonant scattered radiation are indistinguishable except that the latter will be affected by applying a Doppler shift to the system. The scattered intensity will be higher when Mössbauer resonance absorption occurs.

The scattering method uses very similar equipment to that employed in the transmission technique. The only major difference is in the counting geometry. Two examples are shown in Fig. 2.6. The detector must be com-

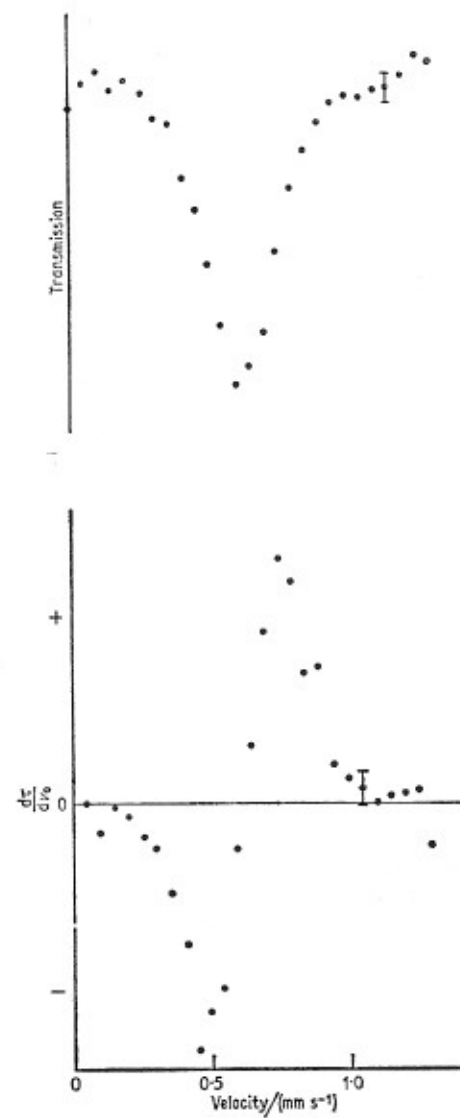


Fig. 2.5 The Mössbauer transmission spectrum of a resonance line and the corresponding derivative spectrum.

pletely shielded from the primary source radiation. The cylindrical and conical scatterers illustrated have been used because of the greater solid

[Refs. on p. 43]

angle which they present without a corresponding increase in the velocity spread. Computation of the effective Doppler shift from the known drive motion can be quite complicated.

The intensity of the scattered radiation is far weaker than the transmitted

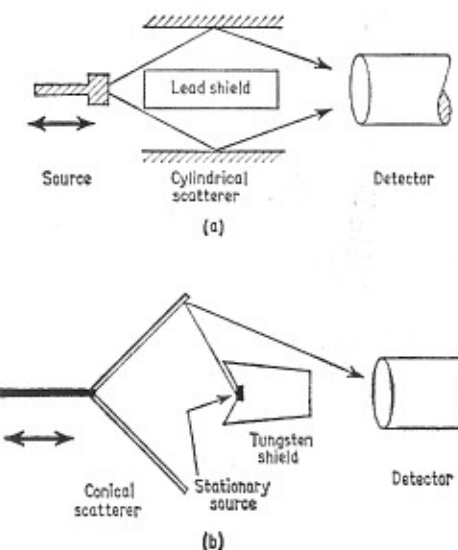


Fig. 2.6 Two types of scattering geometry: (a) using a cylindrical scatterer with a moving source; (b) using a conical moving back-scatterer.

portion and this entails the disadvantage of high-intensity sources. However, the cross-section for resonant scattering can easily be several orders of magnitude higher than that for Rayleigh scattering, giving potentially considerable improvement in signal to noise ratio. This is particularly significant when the recoil-free fraction is very low, and some isotopes such as ^{188}Os (155 keV) have only been observed to give a resonance by scattering methods (see Chapter 16). The technique is also potentially of use for samples which are necessarily too thick for transmission experiments, and when surface states are of particular interest.

One complication which can arise is interference of the recoilless γ -rays with the Rayleigh scattering. Since the interference term shows a phase change at the resonance maximum, a dispersion curve is added to the Mössbauer scattering spectrum causing an asymmetric distortion of the spectrum shape. This can be partially overcome by suitable choice of the scattering angles.

Historically, resonant scattering was first recorded by Barloutaud, Picou, and Tzara [44] in 1960 using ^{119}Sn . Considerable effort has been expended in the study of scattering from the aspect of basic phenomena using metal foils as the scattering materials, but since no chemical application has yet

[Refs. on p. 43]

been made it is only appropriate to mention here a bibliography included in ref. 42. The interference between the Rayleigh and resonant radiation has been observed in ^{57}Fe by Black *et al.* [45, 46]. Of the isotopes where scattering experiments have been reported, ^{186}Os (137.2 keV) and ^{188}Os (155.0 keV) have not been observed by transmission geometry: ^{195}Pt (98.8 keV), ^{182}W (100.1 keV), and ^{186}W (122.6 keV) also have energies above 90 keV. Other Mössbauer resonances which have been studied in the scattering mode are ^{169}Tm (8.4 keV), ^{57}Fe (14.4 keV), ^{119}Sn (23.9 keV), and ^{191}Ir (82.3 keV).

2.6 Source and Absorber Preparation

In this section, some general features concerning the preparation of Mössbauer sources and absorbers will be discussed; details which are specific to individual nuclides are deferred until later chapters, in which each element is considered in turn.

In order to produce a Mössbauer spectrum it is necessary to produce recoil-free γ -photons in quantity. The appropriate excited state of a resonant nucleus can be populated by the prior decay of a radioactive isotope, by nuclear reaction or by excitation. As can be seen by reference to Appendix 1, the most frequent routes to a Mössbauer level are by electron-capture decay (E.C.) for which 37 examples are listed and β^- -decay (46 examples). Some isotopes have an excited state with a long half-life which decays by isomeric transition (I.T.) with γ -ray emission (6 examples). α -emission from ^{241}Am has been used to populate ^{237}Np . Coulombic excitation, that is the bombardment of a target material with very high-energy particles such as oxygen ions has been used for 24 Mössbauer transitions, but has the disadvantage of necessitating *in situ* experimentation because of the effectively instantaneous decay. Nuclear reactions such as (n, γ) and (d, p) which likewise fail to generate a long-lived intermediate (5 transitions) also fall into this category.

The β^- , I.T., and E.C. routes are most conveniently illustrated by the ^{83}Kr decay scheme shown in Fig. 2.7. The details are taken from ref. 47. The isomeric state ^{83m}Kr is produced by the $^{83}\text{Kr}(n, \gamma)^{83m}\text{Kr}$ reaction and has a 1.86-hour half-life. ^{83}Br gives a β^- decay to ^{83m}Kr with a 2.41-hour half-life. ^{83}Rb undergoes E.C. direct to the higher excited states of ^{83}Kr with an 83-day half-life.

The likelihood of success in observing a Mössbauer resonance will depend on numerous factors as follows:

(1) The energy of the γ -ray must be ideally between 10 and 100 keV. This is because γ -rays with energies less than 10 keV are very strongly absorbed in solid matter, and for those above 100 keV the recoil-free fraction which is proportional to $\exp(-E/\gamma^2)$ falls to a very low value (equations 1.3 and 1.12). The absorption cross-section σ_0 is proportional to E_γ^{-2} and also decreases rapidly as E increases. These are the main reasons why the Mössbauer effect

has not yet been recorded for any element lighter than ^{40}K . The energy level separations in light nuclei are usually quite large, and the γ -rays emitted are too energetic to produce a detectable recoil-free fraction. However, as will be seen in later chapters, it is possible to study the chemical bonding effects of light elements in the compounds of those heavier nuclides which do give a Mössbauer resonance.

(2) The half-life of the excited state t_1 should preferably be between about

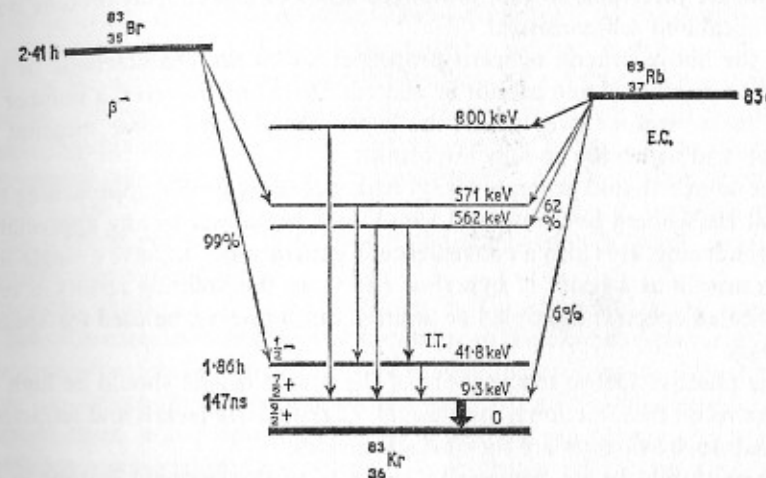


Fig. 2.7 The decay scheme of ^{83}Kr showing how the 9.3-keV Mössbauer level is populated by β^- , I.T., and E.C. decay. The levels are not drawn to scale, and the details are taken from ref. 47.

1 and 100 ns. As we saw in Section 1.3 it is this time which controls the Heisenberg linewidth of the γ -ray energy. If the relative linewidth Γ/E_γ is too narrowly defined (i.e. a long half-life) there are considerable problems in damping out mechanical vibrations in the spectrometer. Conversely, a short lifetime gives a broad line which is difficult to observe and which usually also obscures any chemical hyperfine effects.

(3) The internal conversion coefficient α must be small so that the γ -transition has a high probability of producing a γ -photon rather than a conversion electron. This will also increase the absorption cross-section σ_0 (equation 1.18). Most values listed in Appendix 1 fall in the range 0–10.

(4) The absorption cross-section σ_0 should be large and the free-atom recoil energy E_R should be small. Both of these factors have already been mentioned in connection with other quantities above. Appendix 1 lists 5 transitions for which $\sigma_0 > 10^{-18} \text{ cm}^2$ and few Mössbauer resonances have been observed for transitions in which $\sigma_0 < 0.06 \times 10^{-18} \text{ cm}^2$. Likewise only 5 transitions have a free-atom recoil $E_R > 6 \times 10^{-2} \text{ eV}$ and values are normally in the range $(0.1\text{--}5) \times 10^{-2} \text{ eV}$.

(5) The method of generation of the source γ -rays should ideally be such that a source can be encapsulated and then used for a long period with only the minimum of handling precautions. This implies a long-lived precursor which is easily obtained in high activity, and explains the popularity of those β^- , E.C., and I.T. sources, which can be purchased commercially. The Coulomb, (n, γ), and (d, p) reactions require access to very expensive equipment. For routine chemical applications particularly, sources having lifetimes of months or years are preferable so that prolonged series of experiments become both economical and self-consistent.

All the above criteria concern properties which are characteristic of the transition concerned and cannot be altered. There are, however, a number of other considerations over which the experimentalist has some measure of control, and which are equally important:

(6) The source should generate γ -rays with an energy profile approaching the natural Heisenberg linewidth and should not be subject to any appreciable line broadening. It is also a convenience in general work to have a single-line source unsplit as a result of hyperfine effects, as this splitting results in very complicated spectra; multiple-line sources can, however, be used for special purposes.

(7) The effective Debye temperature of the source matrix should be high so that the recoil-free fraction is substantial. High-melting metals and refractory materials such as oxides are the obvious choices.

(8) There should be no appreciable quantity of the resonant isotope in its ground state in the source, otherwise the self-resonant source term in equation 1.20 becomes important. This will result in an effective source linewidth which is greater than the Heisenberg natural linewidth. In this respect it is interesting to note that the linewidth of a $^{57}\text{Co}/(\text{iron})$ source is greater than that for $^{57}\text{Co}/(\text{iron enriched in } ^{56}\text{Fe})$ because of the greater self-resonance in the former case [48].

(9) Non-resonant scattering inside the source can be reduced, either by careful choice of any other elements in the matrix, or, in the case of metal foils doped with a radioisotope which is the Mössbauer precursor, by controlling the depth to which this generating impurity is diffused.

(10) The ground-state isotope should ideally be stable and have a high natural abundance, otherwise it may become necessary to use artificially enriched compounds at greatly increased cost and inconvenience. Isotopic enrichment is, however, a very important method of improving resolution of spectra and may become essential in work with biological materials or in the study of doped solids where the actual concentration of the element of interest is extremely small.

An important consideration is the chemical effects of the nuclear reactions preceding the occurrence of a Mössbauer event. If, for example, the source preparation involves a long neutron irradiation of the intended source matrix

at high flux as in $^{118}\text{Sn}(n, \gamma)^{119}\text{Sn}$, considerable radiation damage may occur with the formation of lattice defects. Since ideally all the excited atoms should be in identical chemical environments, such defects will result in unwanted line-broadening effects. For this reason it may be desirable either to anneal the source so as to restore the regularity of the crystal lattice, or to extract the radioisotope chemically and then incorporate it in a new matrix.

Very high-energy processes immediately preceding the Mössbauer γ -emission must also be considered. The α -decay of ^{241}Am to give ^{237}Np is sufficiently energetic to displace the daughter nucleus from its initial lattice site. At the same time a considerable number of neighbours are thermally excited. The fact that a Mössbauer spectrum is recorded at all in this case shows that the Np atom comes to rest on a normal lattice site and establishes vibrational integrity with the lattice as a whole in a time which is short compared to the lifetime of the 59.54-keV level, i.e. 63 ns. Complications can occur if the displaced atom is capable of residing on more than one type of chemical site in the crystal.

Similar situations arise, for example, in Coulomb excitation reactions. In the ^{73}Ge case, the low Debye temperature of the Ge metal produces a very low recoil-free fraction. As mentioned in more detail later (p. 109), it is possible to displace the excited atoms completely out of the target material and implant them into a new matrix with a high Debye temperature, thereby obtaining a considerable improvement in the quality of the spectra.

Electron capture involves the incorporation of an inner-shell electron (usually the K-shell) into the nucleus (thereby converting a proton into a neutron and emitting a neutrino). This event is followed by an Auger cascade which results in production of momentary charge states on the atom of up to +7. Many papers on ^{57}Fe experiments have reported the apparent detection of decaying higher charge states resulting from E.C. in ^{57}Co , but as detailed in Chapter 12 it has since been proven that although such states are indeed generated by the after-effects of electron capture, they have already reached stable equilibrium with the solid before the subsequent Mössbauer transition occurs. It would appear that all transient nuclear decay after-effects are over within 10^{-8} of a second. It is important, however, to avoid the production of multiple charge states if the source is not intended to be the subject of a special study designed to detect such states but is to be used only as a source of monochromatic radiation. Some of these topics will be considered in more detail under specific isotopes in later chapters.

Although the preparation of a good source may in some cases be difficult, an adequate absorber can usually be made quite easily. A few general remarks may be useful to illustrate the balance of factors involved, and several texts with full mathematical equations are available [49–52]. Integration of equation 1.20 for simplified cases shows that the measured linewidth will increase

above 2Γ as the absorber thickness increases. This will decrease the resolution of a multiple-line spectrum or the precision with which a single line can be located. Furthermore, an increase in absorber thickness also diminishes the transmission of resonant radiation as a result of non-resonant scattering. However, it is equally clear that the absorber must have a finite thickness for the resonance to be observed at all, hence it follows that there must be an optimum absorber thickness for transmission geometry.

Integration of equation 1.20 for a uniform resonant absorber and an ideally thin source gives the transmission at the resonance maximum as

$$T(0) = e^{-\mu_a t_a} \{ (1 - f_s) + f_s e^{-i T_a} J_0(\frac{1}{2} i T_a) \} \quad 2.1$$

where J_0 is the zero-order Bessel function

$$J_0(ix) = 1 + \left(\frac{x}{2}\right)^2 + \frac{\left(\frac{x}{2}\right)^4}{1^2 \cdot 2^2} + \frac{\left(\frac{x}{2}\right)^6}{1^2 \cdot 2^2 \cdot 3^2} \dots \quad 2.2$$

and $T_a = f_a n_a a_a \sigma_0 t_a$. The function $T(0)$ is plotted in Fig. 2.8 for ^{57}Fe using

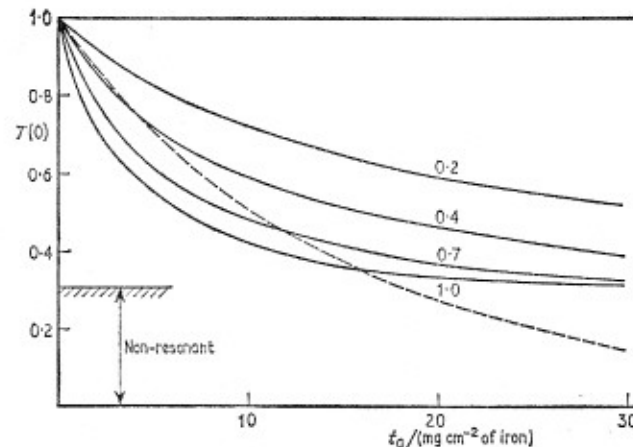


Fig. 2.8 The solid lines are the function $T(0)$ plotted for a zero value of μ_a and four different values of f_a , together with parameters appropriate to ^{57}Fe (14.4 keV). The dashed curve represents the non-resonant attenuation with $\mu_a = 0.067$.

the parameters $\mu_a = 0$ (i.e. no non-resonant scattering), $a_a = 0.0219$, $\sigma_0 = 2.57 \times 10^{-18} \text{ cm}^2$, $f_s = 0.7$ and for f_a values of 0.2, 0.4, 0.7, and 1.0 (the thickness has been converted to mg cm^{-2} of natural iron). The resonant absorption shows a saturation behaviour with increasing thickness. The dashed curve shows the non-resonant scattering attenuation. The quantity to optimise is obviously the absorption in the final transmitted radiation which is $e^{-\mu_a t_a} - T(0) = \Delta T(0)$.

$$\Delta T(0) = e^{-\mu_a t_a} f_s [1 - e^{-i T_a} J_0(\frac{1}{2} i T_a)] \quad 2.3$$

[Refs. on p. 43]

A series of curves for ^{57}Fe with $\mu_a = 0.067$ (the value for natural iron) are shown in Fig. 2.9. The optimum value is seen to be about 10 mg cm^{-2} of

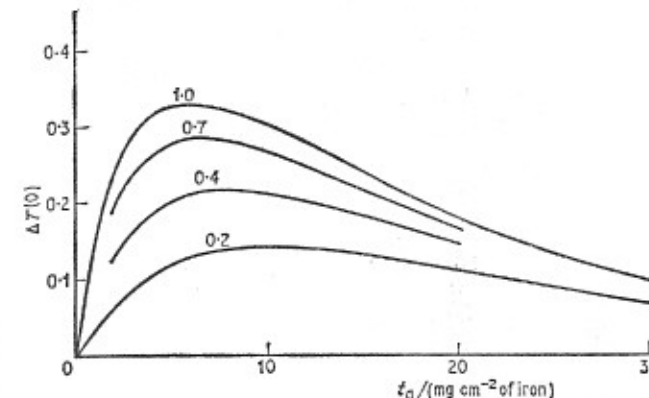


Fig. 2.9 The function $\Delta T(0)$ for ^{57}Fe (14.4 keV) plotted for four values of f_a to show the optimum absorber thickness.

total iron. Fortunately, this value is virtually independent of the recoil-free fraction, a parameter which cannot always be determined in advance. Compounds of iron can be visualised using the same thickness scale, but with a higher non-resonant attenuation coefficient, so that the maximum in the curves moves to lower t_a values.

This type of calculation is only of limited value. The major problem is the possibility of additional non-resonant intensity at the counter produced by the Compton scattering of higher-energy γ -rays. Another factor concerns particle size. The presence of large granules in the absorber can cause a significant reduction in the observed absorption. Calculations [53] show that reduction in particle size eventually results in a reversion to the uniform absorber model.

A discussion of the effects of orientation of the granules and the use of single-crystal absorbers will be deferred until Chapter 3 when the intensities of hyperfine components are discussed.

In general, absorbers can be metal foils, compacted powders, mixtures with inert solid diluents, mixtures with inert greases, frozen liquids, or frozen solutions. The only limitation is on the material used for the windows of the sample container; this must be free of the resonant isotope and have a low mass attenuation coefficient for the γ -ray being studied. Organic plastics and aluminium foil are most commonly used.

2.7 Detection Equipment

Of the four principal types of γ -ray detector used in Mössbauer spectroscopy,

[Refs. on p. 43]

three are conventional instruments and require only brief mention. Further descriptive material and detailed references are readily available [54, 55].

The scintillation-crystal type of detector is frequently used for γ -rays with energies in the range 50–100 keV. A typical example is the NaI/Tl scintillator. The resolution of scintillators deteriorates with decreasing energy of the γ -photon as shown in Fig. 2.10, and such detectors can only be used for very

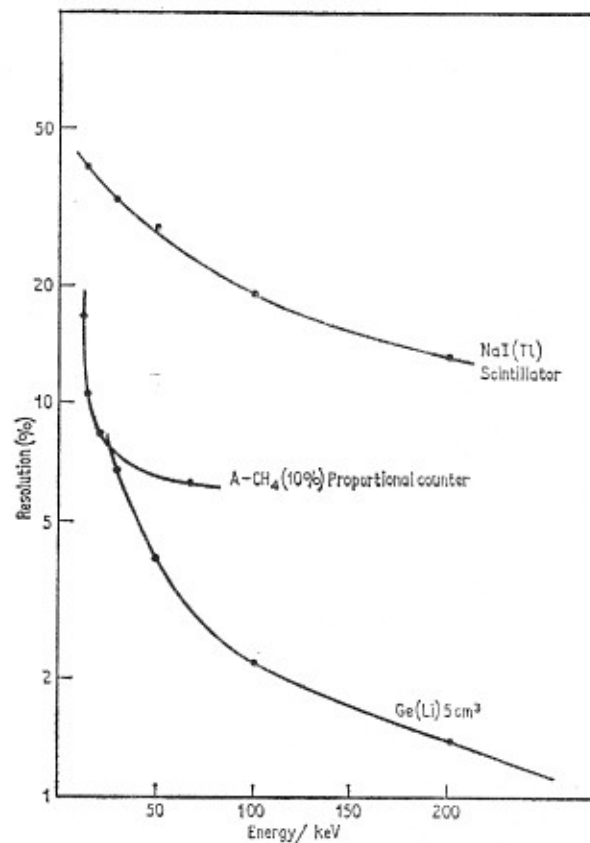


Fig. 2.10 Typical resolution of commonly used γ -ray detectors.

soft γ -rays if the radiation background is low and there are no other X-ray or γ -ray lines with energies near that of the Mössbauer transition. The scintillation unit has a prime advantage of a high efficiency.

Below 40 keV, the gas-filled proportional counter gives better resolution but at the expense of a low efficiency and generally lower reliability. It is possible to lower the radiation background in some cases by the choice of a suitable 'filter'; for example a copper foil will absorb the 27.5- and 31.0-keV ^{125}Te X-rays strongly and transmit most of the 35.5-keV γ -rays because of the higher mass attenuation coefficient for the former.

[Refs. on p. 43]

A more recent development has been the introduction of lithium-drifted germanium detectors. As shown in Fig. 2.10 these give a very highly resolved energy spectrum, but at the expense of low sensitivity, and some inconvenience in use. They are of obvious application where there are several γ -rays of similar energy as often found in the complicated decay schemes of the heavier isotopes. Again the resolution drops drastically with decreasing energy, and they are only of use at the higher end of the Mössbauer energy range. Other drawbacks include a high cost and the necessity for maintaining them indefinitely at liquid nitrogen temperature; irreparable damage results if they are allowed to warm to room temperature.

Comparative examples [56] of the resolution for a source of ^{125}I populating the ^{125}Te 35.5-keV level are given in Fig. 2.11. Although only the Li-drifted Ge crystal gives good resolution of the 35.5 keV γ -ray from the

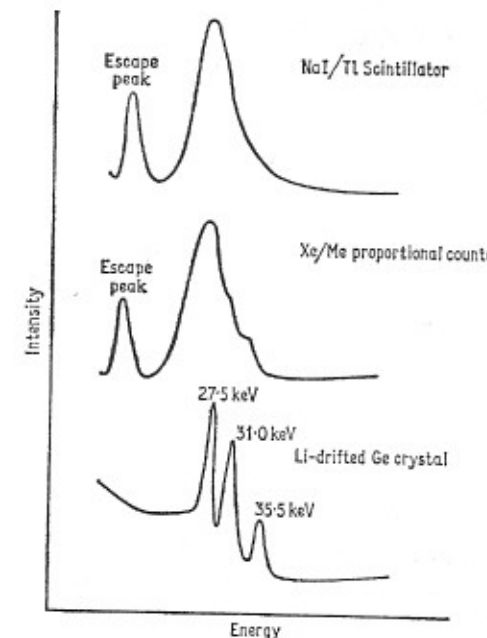


Fig. 2.11 The energy spectrum of an ^{125}I source as recorded with three different detection systems.

27.5- and 31.0-keV X-rays, in this particular instance the other two systems can make use of the 'escape peak' which is produced by loss of an iodine (or xenon) K X-ray from the capturing medium. The tellurium X-rays are too low in energy to generate an escape peak.

The fourth detector system is to use a resonance scintillation counter [57]. A standard type of plastic scintillator for β -detection is doped with the resonant absorber. It is insensitive to the non-resonant background of primary

[Refs. on p. 43]

γ - and X-photons, but will detect the secondary conversion electrons after γ -capture by the resonant nuclei. Although effective, the main difficulty is one of inconvenience, because a new plastic scintillator must be made for each compound used as an absorber. Alternatively, one can use an ordinary Geiger or proportional counter with its inner surface thinly coated with a compound of the isotope being studied [58] or with the proper absorber itself located inside the counter [59]. Again, the recoilless γ -rays are resonantly absorbed by the coating on the internal absorber, and the internal conversion electrons or low-energy X-rays emitted in the subsequent decay of the excited state are then counted with almost 100% efficiency in 4 π -geometry. The counter has been used for ^{57}Fe [59], ^{119}Sn [60], and ^{169}Tm [61], and can be used in principle for any Mössbauer isotope in a compound which has a large recoil-free fraction at room temperature.

Other closely related means of recording a Mössbauer resonance are to record the conversion X-rays scattered from the surface of an absorber [62] or transmitted through it [63], or to count the conversion electrons emitted [64].

2.8 Cryogenic Equipment and Ovens

The very low recoil-free fraction of many γ -ray transitions at ambient temperatures frequently necessitates experimentation at lower temperatures where the Mössbauer effect will be stronger. In addition, the temperature dependence of hyperfine effects is also frequently of interest. If a good source with a high recoil-free fraction at room temperature is available, it may only be necessary to cool the absorber which is stationary. Otherwise, it may be necessary to cool both source and absorber, one of which must also be moving. Standard cryogenic techniques are used [55, 65] and vacuum cryostats are commercially available for work between 4·2 K and 300 K. The two main considerations peculiar to Mössbauer spectroscopy are (a) there must be no vibration inside the cryostat, and (b) there must be a path through the system which is transparent to the γ -rays being studied. Vibration can be eliminated by careful design. It has been found, for example, that a rigid interconnection between a helium container and the outer walls can be made by means of two stacks of several hundred aluminised Mylar washers loosely threaded together, between two nylon washers for support, the large number of contact surfaces lowering the heat transmission to acceptable limits [66]. Cooling the vibrating source as well as the absorber can only be accomplished by inserting the entire transducer unit inside the vacuum space.

Although work below liquid nitrogen temperature necessitates a precision engineered vacuum cryostat, it is quite easy to work between 78 K and 300 K without a vacuum by using styrofoam insulation. Standard coolants are liquid nitrogen (b.p. 77·3 K), liquid hydrogen (b.p. 20·4 K), and liquid helium

[Refs. on p. 43]

(b.p. 4·2 K). Temperatures below these boiling points can also be maintained by pumping on the liquid coolant. Some work calls for more flexible variable-temperature control and in such cases it is possible to use either a temperature gradient along a conducting metal rod regulated by a heating element, or a cold-gas flow technique. Many systems are briefly described in the literature, and there are also some detailed texts available [55, 65, 67-69].

The window material used in vacuum cryostats is usually beryllium, aluminium, or aluminised mylar. It should be noted, however, that commercial beryllium and aluminium often contain sufficient iron to give a detectable ^{57}Fe (14 keV) resonance, and this has been known to cause problems when working with this isotope.

Temperatures above 300 K are sometimes desirable for ^{57}Fe work, and a controlled-temperature furnace is then required [68, 69]. The sample is frequently sandwiched between thin discs of beryllium, graphite, or aluminium (m.p. 660°C) attached to an electric heating coil in a vacuum. Alternatively [70], the sample can be placed in a furnace with thin entrance and exit windows and containing an atmosphere of hydrogen to prevent oxidation. A vacuum furnace capable of providing temperatures up to 1000°C has been described [71] and temperatures of 1700°C have been reached with a helium-filled oven with beryllium windows [72].

High-pressure work has been published by relatively few laboratories because pressure cells require special experience and engineering [73-75].

If a large external magnetic field is to be applied to an absorber, this is usually done with a superconducting magnet installation which also requires a liquid helium cryostat for its operation [76]. Again, several commercial instruments are available.

2.9 Velocity Calibration

One of the more difficult experimental aspects of Mössbauer spectroscopy is the accurate determination of the absolute velocity of the drive. The calibration is comparatively easy for constant-velocity instruments, but most spectrometers now use constant-acceleration drives. The least expensive method, and therefore that commonly used, is to utilise the spectrum of a compound which has been calibrated as a reference. Unfortunately, suitable international standards and criteria for calibration have yet to be decided. As a result, major discrepancies sometimes appear in the results from different laboratories. The problem is accentuated by having figures quoted with respect to several different standards, necessitating conversion of data before comparison can be made. However, calibration of data from an arbitrary standard spectrum will at least give self-consistency within each laboratory.

Several systems for a more direct absolute-velocity calibration have been developed. In one such method [31], the output of the monitoring pick-up

[Refs. on p. 43]

coil is fed to a voltage-to-frequency converter and thence to the time-mode multichannel analyser as a train of pulses with the same frequency. The counting rate in a channel is thus a function of the instantaneous velocity, provided of course that the linearities of the pick-up coil and the voltage-to-frequency converter are both accurate. This method gives a good check on

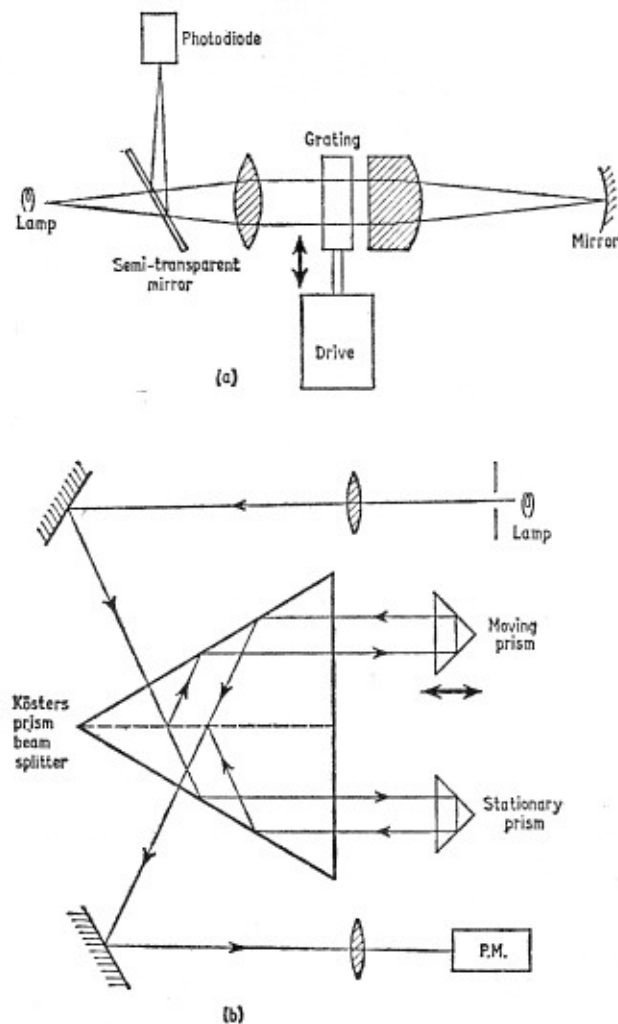


Fig. 2.12 Absolute calibration of constant-acceleration drives using (a) diffraction grating, (b) optical interferometer.

the day-to-day linearity and stability of the drive, but is not easily calibrated in absolute terms from a known hyperfine spectrum.

An absolute calibration can be obtained by mounting a diffraction grating

[Refs. on p. 43]

(typically 8 μm spacing) on the reverse end of the source drive-shaft [77]. Reflection of the diffraction image will produce a light intensity which is periodic by interference because of the varying velocity of the grating. The fluctuations can be detected and converted to pulses which after accumulation in the time-mode analyser give a calibration similar to that mentioned above. The basic components are illustrated schematically in Fig. 2.12a. The absolute accuracy is claimed to be as good as that of the best mechanical drives.

A similar method uses an optical interferometer as illustrated in Fig. 2.12b [78]. The motion of the small prism, which is attached to the drive, causes a time-dependent interference which is again converted to pulses and registered in the analyser. Neither method is widely applicable because of the prohibitive cost of the precision optical equipment.

Calibration in terms of a known frequency has also been accomplished by mounting the absorber on a quartz crystal and calculating the velocity scale from the spectrum sidebands produced by frequency modulation [79].

2.10 Curve Fitting by Computer

Much of the Mössbauer spectroscopic data which is published comes from institutions which also have large computer facilities. Since the raw data of a spectrum are already digitised, it is in a very convenient form for automated analysis by digital computer. The majority of multichannel analysers have output signals which are either directly compatible with or easily adapted for appropriate types of punched paper tape or magnetic tape units, so that accumulated spectra can be printed out in a form which is compatible with the computer installation.

The information which may be required from the computer analysis of the data are the parameters of a selected function which are the best possible fit to the observed spectrum. In the simplest cases this function will be one or more Lorentzian curves. However, more complex types of function may sometimes be required, for example when fitting multi-line spectra which are subject to motional narrowing (see p. 72).

The general problem can be described as follows. The data comprise N digitised values Y_i . The function which is to be fitted contains n variables, represented by the vector V , and will give a calculated value at data point i of $A(V)_i$. The error thereby incurred is

$$e_i = Y_i - A(V)_i \quad 2.4$$

The best possible fit to the N data points, which is the answer required, must be such that the overall error is a minimum. The statistics of radioactive counting processes [80] tell us that the values of Y_i will be distributed as a Poisson distribution with a variance equal to the mean, and hence the standard deviation in Y_i is $\sqrt{Y_i}$. The quantity to be minimised for a best fit is

[Refs. on p. 43]

therefore the 'goodness of fit' function

$$F(V) = \sum_{i=1}^N \left\{ \frac{[Y_i - A(V)_i]^2}{Y_i} \right\} \quad 2.5$$

which at the minimum is a chi-squared function and can be used to determine the probability of the fit being a valid one.

Equation 2.5 is non-linear in the variables V and represents a complex mathematical problem even for high-speed digital computers. Considerable effort has been expended since 1959 in developing appropriate methods, and their application to Mössbauer spectroscopy has been specifically detailed in several papers [80-82].

The chi-squared (χ^2) function, $F(V)$, has $N - n$ degrees of freedom, and the validity of the result can be determined from standard tables [83]. As a general rule, the statistical significance of the fit decreases rapidly as $F(V)$ rises in value. For example, a computed fit with 400 degrees of freedom is within the 25-75% confidence limits of a χ^2 distribution if $380 < F(V) < 419$, and within the 5-95% limits if $355 < F(V) < 448$.

The χ^2 values obtained in Mössbauer spectroscopy are frequently higher than one would expect because the function used is not absolutely correct. Thus, peaks may not be strictly Lorentzian in shape, as in cases of order-disorder phenomena where they may be distorted by a large number of small variations in the electronic state of the absorbing atoms due to environment fluctuations. Again, if the counting rate is greater than about 10^5 counts per second in the detection system the 'dead-time' effects which occur in the instrumentation will distort the Poisson distribution. In this case the total registered count-rate could still be low if the rejection fraction at the single-channel discriminator were high. Other factors which affect the χ^2 values include instrumental drift, counting geometry, cosine effects, and the proportion of the spectrum being computed which is zero-absorption baseline.

Introducing additional variables will invariably lower the value of $F(V)$, but the decrease may not be large enough to justify the new fit. The final decision regarding the valid interpretation of the data must and should remain with the experimenter, using his full experience and chemical knowledge.

One useful feature of some of the mathematical methods of solution is that they also provide information on the precision of the final values of the variables [80], but the effects of instrument drift are likely to be underestimated as it is assumed that the velocity of any given channel is not a function of time.

Although data are usually analysed by specifying an exact mathematical function, it is possible (with slightly different methods) to use an experimentally defined peak-shape if the former is not known with precision [84].

One obvious development of these various methods is the application of

direct on-line time-sharing computer techniques. In principle, this enables the analyser output to be transmitted directly to the central processing unit from the laboratory, and the results of the calculation can then be returned at least in abbreviated form to a remote terminal for rapid preliminary assessment of the experiment.

REFERENCES

- [1] R. L. Mössbauer, *Z. Physik*, 1958, **151**, 124.
- [2] R. L. Mössbauer, *Naturwiss.*, 1958, **45**, 538.
- [3] K. Cassell and A. H. Jiggins, *J. Sci. Instr.*, 1967, **44**, 212.
- [4] R. Booth and C. E. Violet, *Nuclear Instr. Methods*, 1963, **25**, 1.
- [5] C. E. Johnson, W. Marshall, and G. J. Perlow, *Phys. Rev.*, 1962, **126**, 1503.
- [6] C. W. Kocher, *Rev. Sci. Instr.*, 1965, **36**, 1018.
- [7] A. J. Bearden, M. G. Hauser, and P. L. Mattern, 'Mössbauer Effect Methodology Vol. 1', Ed. I. J. Gruverman, Plenum Press, N.Y., 1965, p. 67.
- [8] H. M. Kappler, A. Trautwein, A. Mayer, and H. Vogel, *Nuclear Instr. Methods*, 1967, **53**, 157.
- [9] P. A. Flinn, *Rev. Sci. Instr.*, 1963, **34**, 1422.
- [10] P. Flinn, 'Mössbauer Effect Methodology Vol. 1', Ed. I. J. Gruverman, Plenum Press, N.Y., 1965, p. 75.
- [11] J. Lipkin, B. Schechter, S. Shtrikman, and D. Treves, *Rev. Sci. Instr.*, 1964, **35**, 1336.
- [12] F. W. D. Woodhams, *J. Sci. Instr.*, 1967, **44**, 285.
- [13] V. P. Al'fimenkov, Yu. M. Ostanevich, T. Ruskov, A. V. Strelkov, F. L. Shapiro, and W. K. Yen, *Soviet Physics - J.E.T.P.*, 1962, **15**, 713 (*Zhur. eksp. teor. Fiz.*, 1962, **42**, 1029).
- [14] R. C. Knauer and J. G. Mullen, *Rev. Sci. Instr.*, 1967, **38**, 1624.
- [15] P. E. Clark, A. W. Nichol, and J. S. Carlow, *J. Sci. Instr.*, 1967, **44**, 1001.
- [16] J. Pahor, D. Kelsin, A. Kodre, D. Hanzel, and A. Moljk, *Nuclear Instr. Methods*, 1967, **46**, 289.
- [17] Y. Hazony, *Rev. Sci. Instr.*, 1967, **38**, 1760.
- [18] D. St P. Bunbury, *J. Sci. Instr.*, 1966, **43**, 783.
- [19] R. Zane, *Nuclear Instr. Methods*, 1966, **43**, 333.
- [20] D. Rubin, *Rev. Sci. Instr.*, 1962, **33**, 1358.
- [21] R. L. Cohen, *Rev. Sci. Instr.*, 1966, **37**, 957.
- [22] R. L. Cohen, P. G. McMullin, and G. K. Wertheim, *Rev. Sci. Instr.*, 1963, **34**, 671.
- [23] V. Vali and T. W. Nybakken, *Rev. Sci. Instr.*, 1964, **35**, 1085.
- [24] R. Gerson and W. S. Denno, *Rev. Sci. Instr.*, 1965, **36**, 1344.
- [25] L. Lovborg, *Nuclear Instr. Methods*, 1965, **34**, 307.
- [26] M. Bornaz, G. Filoti, A. Gelberg, V. Grabari, and C. Nistor, *Nuclear Instr. Methods*, 1966, **40**, 61.
- [27] J. D. Cooper, T. C. Gibb, N. N. Greenwood, and R. V. Parish, *Trans. Faraday Soc.*, 1964, **60**, 2097.
- [28] J. D. Cooper and N. N. Greenwood, *J. Sci. Instr.*, 1966, **43**, 71.
- [29] C. A. Miller and J. H. Broadhurst, *Nuclear Instr. Methods*, 1965, **36**, 283.
- [30] T. E. Cranshaw, *Nuclear Instr. Methods*, 1964, **30**, 101.

- [31] F. C. Ruegg, J. J. Spijkerman, and J. R. de Voe, *Rev. Sci. Instr.*, 1965, **36**, 356.
- [32] E. Kankeleit, *Rev. Sci. Instr.*, 1964, **35**, 194.
- [33] Y. Reggev, S. Bukshpan, M. Pasternak, and D. A. Segal, *Nuclear Instr. Methods*, 1967, **52**, 193.
- [34] E. Nadav and M. Palmai, *Nuclear Instr. Methods*, 1967, **56**, 165.
- [35] M. Michalski, J. Piekoszewskii, and A. Sawicki, *Nuclear Instr. Methods*, 1967, **48**, 349.
- [36] R. H. Goodman and J. E. Richardson, *Rev. Sci. Instr.*, 1966, **37**, 283.
- [37] R. H. Goodman, 'Mössbauer Effect Methodology Vol. 3', Ed. I. J. Gruverman, Plenum Press, N.Y., 1967, p. 163.
- [38] J. E. S. Bradley and J. Marks, *Nature*, 1961, **192**, 1176.
- [39] T. Bressani, P. Brovetto, and E. Chiavassa, *Phys. Letters*, 1966, **21**, 299; *Nuclear Instr. Methods*, 1967, **47**, 164.
- [40] H. Frauenfelder, 'The Mössbauer Effect', W. A. Benjamin, Inc., N.Y., 1962.
- [41] A. J. F. Boyle and H. E. Hall, *Repts. Progr. in Physics*, 1962, **25**, 441.
- [42] J. K. Major, 'Mössbauer Effect Methodology Vol. 1', Ed. I. J. Gruverman, Plenum Press, N.Y., 1965, p. 89.
- [43] P. Debrunner, 'Mössbauer Effect Methodology Vol. 1', Ed. I. J. Gruverman, Plenum Press, N.Y., 1965, p. 97.
- [44] R. Barloutaud, J-L. Picou, and C. Tzara, *Compt. rend.*, 1960, **250**, 2705.
- [45] P. J. Black, D. E. Evans, and D. A. O'Connor, *Proc. Roy. Soc.*, 1962, A²⁷⁰, 168.
- [46] P. J. Black, G. Longworth, and D. A. O'Connor, *Proc. Phys. Soc.*, 1964, **83**, 925.
- [47] C. M. Lederer, J. M. Hollander, and I. Perlman, 'Table of Isotopes - 6th Ed.', John Wiley & Sons, Inc., N.Y., 1967.
- [48] G. A. Chackett, K. F. Chackett, and B. Singh, *J. Inorg. Nuclear Chem.*, 1960, **14**, 138.
- [49] S. L. Ruby and J. M. Hicks, *Rev. Sci. Instr.*, 1962, **33**, 27.
- [50] D. A. O'Connor, *Nuclear Instr. Methods*, 1963, **21**, 318.
- [51] S. Margulies and J. R. Ehrman, *Nuclear Instr. Methods*, 1961, **12**, 131.
- [52] S. Margulies, P. Debrunner, and H. Frauenfelder, *Nuclear Instr. Methods*, 1963, **21**, 217.
- [53] J. D. Bowman, E. Kankeleit, E. N. Kaufmann, and B. Persson, *Nuclear Instr. Methods*, 1967, **50**, 13.
- [54] K. Siegbahn (Ed.), 'Alpha, Beta, and Gamma Ray Spectroscopy', North Holland Publ., Amsterdam, 1965.
- [55] N. Benczer-Koller and R. H. Herber, Chap. 2, 'Experimental Methods' in V. I. Goldanskii and R. H. Herber (Eds.), 'Chemical Applications of Mössbauer Spectroscopy', Academic Press, New York, 1968.
- [56] C. E. Violet, 'The Mössbauer Effect and its Appl. to Chem.', *Adv. Chem. Ser.* 1967, **68**, Chap. 10.
- [57] L. Levy, L. Mitrani, and S. Ormandjiev, *Nuclear Instr. Methods*, 1964, **36**, 233.
- [58] K. P. Mitrofanov and V. S. Shpinel, *Zhur. eksp. teor. Fiz.*, 1961, **40**, 983.
- [59] D. A. O'Connor, N. M. Butt, and A. S. Chohan, *Rev. Mod. Phys.*, 1964, **A 361**.
- [60] K. P. Mitrofanov, N. V. Illarionova, and V. S. Shpinel, *Pribory i Tekhnika Eksperim.*, 1963, **8**, 49; English Transl. in *Instr. Exptl. Tech. USSR*, 1963, **3**, 415.
- [61] J. S. Eck, N. Hershkowitz, and J. C. Walker, *Bull. Am. Phys. Soc.*, 1965, **10**, 571.

- [62] H. Frauenfelder, D. R. F. Cochran, D. E. Nagle, and R. D. Taylor, *Nuovo Cimento*, 1961, **19**, 183.
- [63] N. Hershkowitz and J. C. Walker, *Nuclear Instr. Methods*, 1967, **53**, 273.
- [64] E. Kankeleit, *Z. Physik*, 1961, **164**, 442.
- [65] M. Kalvius, 'Mössbauer Effect Methodology Vol. 1', Ed. I. J. Gruverman, Plenum Press, N.Y., 1965, p. 163.
- [66] D. P. Johnson, G. A. Erickson, and J. G. Dash, *Rev. Sci. Instr.*, 1968, **39**, 420.
- [67] A. J. Nozik and M. Kaplan, *Anal. Chem.*, 1967, **39**, 854.
- [68] F. Van der Woude and G. Boom, *Rev. Sci. Instr.*, 1965, **36**, 800.
- [69] B. Sharon and D. Treves, *Rev. Sci. Instr.*, 1966, **37**, 1252.
- [70] D. E. Nagle, H. Frauenfelder, R. D. Taylor, D. R. F. Cochran, and B. T. Matthias, *Phys. Rev. Letters*, 1960, **5**, 364.
- [71] R. S. Preston, S. S. Hanna, and J. Heberle, *Phys. Rev.*, 1962, **128**, 2207.
- [72] R. G. Barnes, R. L. Mössbauer, E. Kankeleit, and J. M. Poindexter, *Phys. Rev.*, 1964, **136**, A 175.
- [73] R. Ingalls, 'Mössbauer Effect Methodology Vol. 1', Ed. I. J. Gruverman, Plenum Press, N.Y., 1965, p. 185.
- [74] D. Pipkorn, C. K. Edge, P. Debrunner, G. de Pasquali, H. G. Drickamer, and H. Frauenfelder, *Phys. Rev.*, 1964, **135**, A 1604.
- [75] P. Debrunner, R. W. Vaughan, A. R. Champion, J. Cohen, J. A. Moyzis, and H. G. Drickamer, *Rev. Sci. Instr.*, 1966, **37**, 1310.
- [76] J. Heberle, 'Mössbauer Effect Methodology Vol. 2', Ed. I. J. Gruverman, Plenum Press, N.Y., 1966, p. 95.
- [77] H. de Waard, *Rev. Sci. Instr.*, 1965, **36**, 1728.
- [78] J. J. Spijkerman, F. C. Ruegg, and J. R. De Voe, International Atomic Energy Agency Technical Reports Series No. 50, Vienna, 1966, p. 53.
- [79] T. E. Cranshaw and P. Reivari, *Proc. Phys. Soc.*, 1967, **90**, 1059.
- [80] B. J. Duke and T. C. Gibb, *J. Chem. Soc. (A)*, 1967, 1478.
- [81] S. W. Marshall, J. A. Nelson, and R. M. Wilenzick, *Comm. Assoc. Computing Machinery*, 1965, **8**, 313.
- [82] G. M. Bancroft, A. G. Maddock, W. K. Ong, R. H. Prince, and A. J. Stone, *J. Chem. Soc. (A)*, 1967, 1966.
- [83] D. B. Owen, 'Handbook of Statistical Tables', Pergamon Press, 1962.
- [84] A. Gavron, D. Kedem, and T. Rothen, *Nuclear Instr. Methods*, 1968, **61**, 213.